

POLITECNICO DI TORINO  
Repository ISTITUZIONALE

Research on the Automobile Aerodynamic Field at the Politecnico di Torino in the Second Half of the Twentieth Century

*Original*

Research on the Automobile Aerodynamic Field at the Politecnico di Torino in the Second Half of the Twentieth Century / Nuccio, Patrizio. - In: SAE TECHNICAL PAPER. - ISSN 0148-7191. - ELETTRONICO. - 1:(2023). (Intervento presentato al convegno WCX SAE World Congress Experience tenutosi a Detroit) [10.4271/2023-01-0015].

*Availability:*

This version is available at: 11583/2978384 since: 2023-05-08T08:18:55Z

*Publisher:*

SAE

*Published*

DOI:10.4271/2023-01-0015

*Terms of use:*

This article is made available under terms and conditions as specified in the corresponding bibliographic description in the repository

*Publisher copyright*

GENERIC -- per es. EPJ (European Physical Journal) : quando richiesto un rinvio generico specifico per

This is a post-peer-review, pre-copyedit version of an article published in SAE TECHNICAL PAPER. The final authenticated version is available online at: <http://dx.doi.org/10.4271/2023-01-0015>

(Article begins on next page)

# Research on the Automobile Aerodynamic Field at the Politecnico di Torino in the Second Half of The Twentieth Century

**Patrizio Nuccio**

Politecnico di Torino Energy Department

## Abstract

With this paper the author first of all wants to honor the memory of Professor Alberto Morelli with whom I had the privilege of working for many years at the Politecnico di Torino. Morelli radically changed the way of designing car body shapes, while bringing the aspect of reducing the aerodynamic resistance of a vehicle to the attention of car designers. Morelli's research activity began in the early 1950s and, between the 1950s and 1960s, he designed and built a number of car prototypes, whose coefficient of aerodynamic resistance was substantially reduced compared to that of the cars of that time, sometimes resorting to revolutionary architectures such as a "diamond" arrangement of the wheels. A fundamental step of Morelli's research in the field of vehicle aerodynamics was the Pininfarina full-scale wind tunnel project, which was set up between the end of the 1960s and the beginning of the 1970s, and was inaugurated in 1972: fifty years have therefore passed since that occasion. An impressive result, obtained in the second half of the 1970s, was the maquette of the Pininfarina-CNR car, which had front air intakes, internal flows as well as other external details, such as rear-view mirrors: in this case, the  $C_x$  value was 0.20. His activity continued with significant results in the field of car aerodynamics, in particular concerning the interaction between the wakes of the car and of the wheels.

## Introduction

The aim of this paper is to present the research activity conducted by Professor Alberto Morelli at the Politecnico di Torino from the 1950s until his death. About twenty years after his death, this contribution should be considered as a way of honoring his memory. The author, having had the privilege of collaborating with Professor Morelli in some of his research activities and of teaching with him, would like to recall how much he contributed to the development and advancement of techniques in the automotive field.

Alberto Morelli's research activity in both the automotive and aeronautical fields began in the early 1950s. His experience in the latter field, which consisted in the design and construction of seven gliders for the Gliding Center at the Politecnico di Torino, played an important role in all of his subsequent research activities conducted to improve vehicles from an aerodynamic point of view. I would therefore first like to present some details of about twenty years of Prof. Alberto Morelli's activities as a glider designer at the Gliding Center at the Politecnico di Torino, not because it occurred before his research in the automotive field (it was actually contextual), but because it surely influenced his research in the car aerodynamics field to a great extent.

The Gliding Center was founded in May 1952. In over twenty years of intense activity, the center designed and built seven prototype gliders. Two of these gliders were mass-produced in Italy and in France, respectively.

But it is *Veltro* glider that in particular deserves mentioning [1]. The *Veltro* was built in just eight months, and its first flight took place in July 1954. This glider, as is evident from a comparison with the general architecture of today's gliders, made huge advancements, as can be seen in Figure 1.

A high degree of tapering of the wing, which allowed the induced drag to be drastically reduced, can be observed in the figure: the reduction of this aerodynamic resistance component was also fundamental in obtaining low aerodynamic drag in motor vehicles.

The glider's performance was high at both low and high speeds: for example, the maximum glide ratio was 35, about 21% more than similar gliders of that time with the same 15 m wingspan.



Figure 1. Comparison of the *Veltro* built in 1954 shown at the Italia '61 Exposition (above) and one of today's gliders (below): the similarity is obvious. The '61 Exhibition took place in Turin and was organized to celebrate the centenary of the Unification of Italy

Thanks to the significant innovations he introduced, the *Veltro*, piloted by Morelli himself, achieved the best performance in Italy at that time: an absolute altitude of over 7000 m in March of 1956 and 300 km of free-distance in August of 1957.

The extraordinary progress achieved by Morelli, until his death in 2004 at the age of 76, in reducing the aerodynamic drag of motor vehicles will now be presented in the following sections.

## The first studies conducted to obtain a body of minimum drag moving in the vicinity of the ground

The first experimental car, M1000, which Morelli designed and built from 1953 to 1956, was the result of his first analytical studies, made in the early fifties and summarized in one of his publications [2]. These studies highlighted the effect of different parameters on the aerodynamic drag coefficient  $C_x$  of basic bodies tested at a 1:5 scale in a wind tunnel (Figure 2) as a function of the relative distance " $d = h/b$ " from the ground (where  $h$  is the distance from the ground and  $b$  is the maximum width of the body), of the center-line camber " $i$ " (ratio between the maximum distance of centerline " $c$ " and cord " $l$ ") and the incidence " $\alpha$ " (angle between the undisturbed air-speed and the chord) (Figure 3,4). According to the standard SAE nomenclature for aerodynamic coefficients, hereafter  $C_x$  and  $C_z$  correspond to the drag coefficient  $C_D$  and to the lift coefficient  $C_L$ .

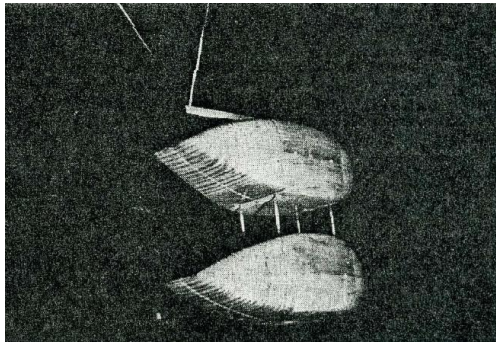


Figure 2. Basic body tested in 1:5 at a scale in the wind tunnel. The image method was used on a scaled-down model in order to simulate the effect of the ground [2]

Therefore, Morelli designed the M1000 with appropriate values for height " $h$ " from the ground, for center line camber " $i$ " and incidence

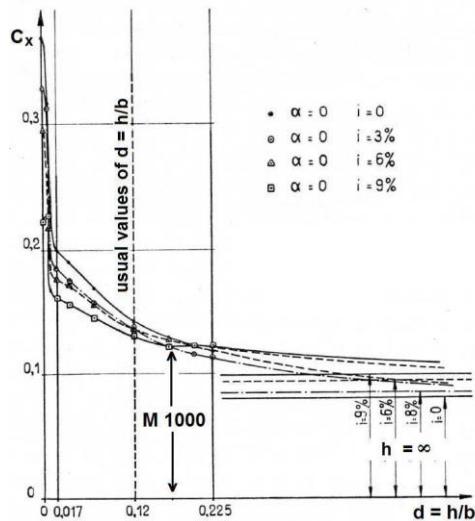


Figure 3. Effect of the relative distance from the ground " $d$ " =  $h/b$  and of camber line " $i$ " on the  $C_x$  of a drop shape. The  $h/b$  value of M1000 is also shown (about 0.17) [2]

" $\alpha$ " of the reference axis, as Figure 3 shows, where it is clear that the highest possible " $d$ " value is appropriate. However, he also took into consideration the rounding of the front and rear parts of the vehicle, as well as the wheel-mudguard covering and underside-floor protection (see Figure 4 for longitudinal views of the M1000 car).

The M1000  $C_x$  value, measured in the wind tunnel at the Politecnico di Torino on a 1:5 scale model, showed a value of 0.102, while the value determined on the road and on the test-bench was  $0.14 \pm 0.02$ . As far as the experimental tests are concerned, an image method was also used on the scaled-down model shown in the first picture in Figure 5 (above) in order to simulate the effect of the ground. The second picture in Figure 5 (below) instead shows the M1000 car being tested, in 1977, in the Pininfarina full-scale wind tunnel: in this case the  $C_x$  was 0.295. This difference from the 1:5 scale model was the result of a very different Reynolds number with respect to the "full scale" vehicle. The results of these first experimental tests on small-scale models in the wind tunnel probably convinced Alberto Morelli that it was

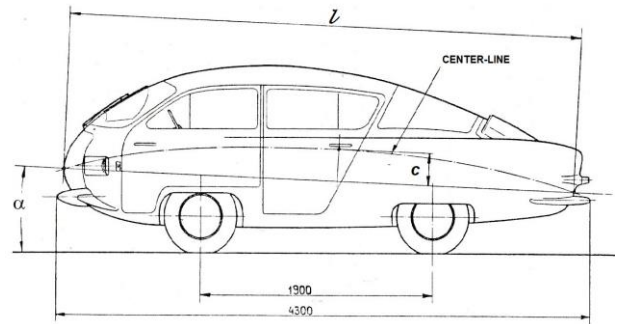


Figure 5. The M1000 model in the wind-tunnel at the Politecnico di Torino in 1953 (above) and a full-scale car in the Pininfarina wind-tunnel in 1977, where a  $C_x = 0.295$  was found (below)

necessary to carry out tests on vehicles at a 1:1 scale, or even slightly less. The project for a full scale wind tunnel was in fact started about ten years later as well as a more detailed study of wheel aerodynamics. Finally, a comparison of experimental values of  $C_x$ , as measured in the wind tunnel for different car models is shown in Figure 6: The M1000 presented a  $C_x$  coefficient that was on average about 35% lower than that of medium-size sedan cars of the same period, that is, 1956. The

same figure also shows the  $C_x$  of some other Pininfarina cars (that is, the PF"X", PF"Y", Pininfarina CNR) which were designed by Morelli in the following years and which will be presented and discussed later on.

– Low cost: the PF"X" was simplified, with respect to a traditional vehicle, as far as the structure of the body is concerned, as there was practically no torsion of the body. Moreover, the steering mechanism was limited to the front wheel, while the transmission of motion was left to the rear wheel (Figure 7), no differential was present and, finally, the

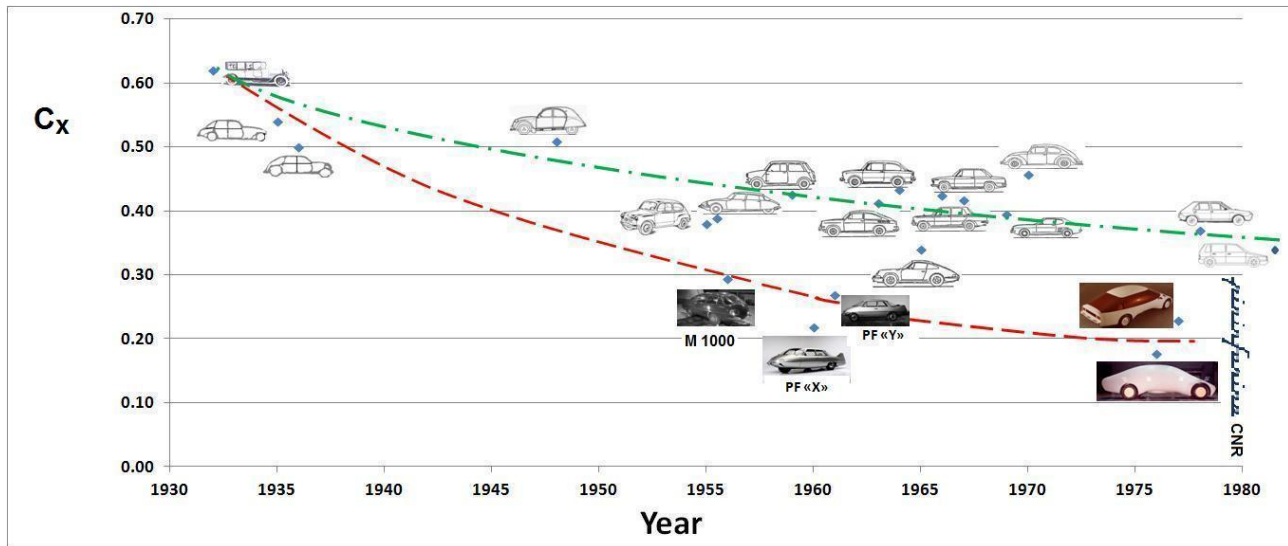


Figure 6. Comparison of the experimental values of the  $C_x$  of M1000 measured in a wind tunnel and those of different car models. The values of the PF"X", PF"Y" and Pininfarina CNR car models made in the subsequent years are also shown

## The car prototypes designed for Pininfarina

### The PF"X" car

The car Morelli designed after the M1000, was the PF"X", which was built by Pininfarina (Figure 7) and presented at the 42nd International Motor Show in Turin and in Brussels in 1960.

A rhomboid arrangement of the wheels was chosen for this vehicle because it was more suitable than the previous traditional aerodynamically shaped one. In fact, with its four wheels arranged in a diamond shape, the aerodynamic PF"X" had a drag coefficient of 0.219, thus indicating that it was much more advanced than the other cars of the same era, as Figure 6 shows. However, this unusual wheel arrangement was also chosen because of its mechanical and structural simplification, which was achieved without sacrificing speed or economy, capacity or maneuverability, low cost or comfort. In reference [3], Alberto Morelli emphasized these advantages of the PF"X" vehicle:

- High speed and operating economy: these characteristics were achieved by means of a very low aerodynamic drag which allowed a reduction of fuel consumption to be achieved, in particular during highway and extra-urban driving.
- Roominess: the volume in the PF"X" passenger vehicle, which was intended to accommodate 4-5 people, was equal to 81% of the total volume, while the passenger compartment in a conventional vehicle with the same total volume was 70%, with an equivalent volume of the luggage compartment.
- Maneuverability: the rounded shape of the front allowed the vehicle to be parked more easily, even though the PF"X" vehicle was longer than traditional vehicles of that era. Another important aspect concerns the kinematics of the movement: during steering maneuvers, the PF"X" vehicle reached higher maximum angular acceleration values than an equivalent traditional vehicle, i.e. of about 24%, thanks to the reduced distance between the front axis and the center of rotation of the vehicle.

emergency brake was only on the front wheel. All this led to a weight reduction of about 10%, compared to an equivalent traditional car.

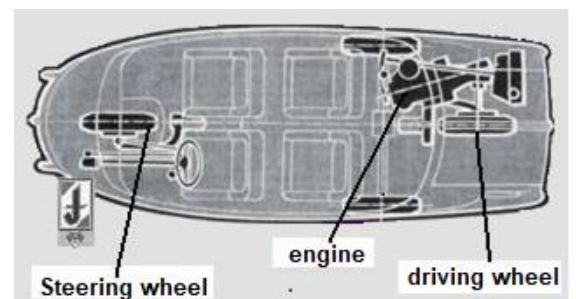


Figure 7. The Pininfarina PF"X" car (above) and schema of the arrangement of the mechanical parts (below) [3]

- Comfort: since the pitch and roll motions only involved two wheels, there was a reduction in the oscillation periods during both motions and thus a corresponding increase in flexibility. The greater pitching due to braking in the PFX vehicle was contrasted with anti-dive suspension kinematics.



## Cornering and braking behavior of a vehicle with a rhomboidal wheel arrangement

Morelli also theoretically predicted the behavior of such a vehicle under steering and braking conditions [4]. Figure 8 shows the “delta” difference between the medium slip angle of the central and rear wheels,  $\Delta_R$ , and the front one,  $\Delta_A$ , vs the overall adhesion coefficient,  $A_c$ , necessary to balance the centrifugal force during steering. Since the front wheelbase was much larger than the rear wheelbase, the central wheels and the rear wheel were reduced to a single hypothetical wheel that was suitably positioned between the central and rear axles. In the case of  $\Delta = 0$ , the vehicle was in neutral, if  $\Delta > 0$ , oversteering occurred, if  $\Delta < 0$ , as shown in Figure 8, from the calculation results, the PF”X” vehicle was almost in neutral up to an  $A_c$  value equal to 0.6, after which it began to be over-steered and to lose grip. It was also observed, in the presence of steering and braking, that the adhesion coefficients of a single wheel with a high limit of the overall braking coefficient led to situations without oversteering problems or to an intermediate condition between understeering and oversteering. These theoretical results were also confirmed through experimental tests on the PF”X” vehicle on the road. The head-tail phenomenon never occurred in any of the tests, even with braking at the grip limit.

### The PF ”Y” car

As the architecture of PF”X” was considered too “revolutionary”, in

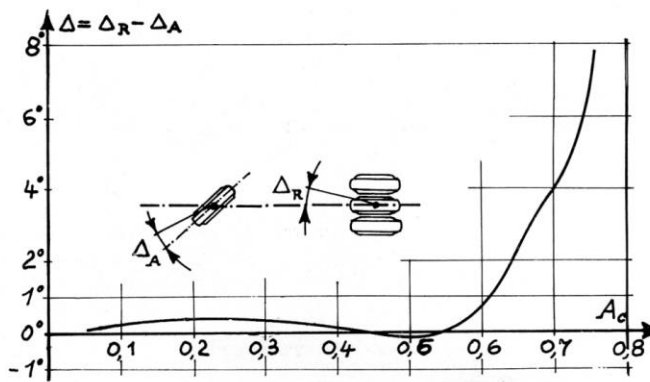


Figure 8. The  $\Delta$  difference between the medium slip angle of the central and rear wheels  $\Delta_R$  and the front one  $\Delta_A$  vs the overall centrifugal adhesion coefficient  $A_c$  without braking forces (the central wheels and the rear wheel are reduced to one single wheel) [4]

1961 Alberto Morelli designed a new vehicle for Pininfarina, that is, Project “Y”, which had conventional wheel locations and was based on the same mechanical solutions as the Fiat 600D (Figure 9 above). This vehicle had a 0.27 higher  $C_x$  than PF”X”, but this value was still lower than the  $C_x$  values of between 0.4 and 0.45 of that period (Figure 6). In the first version of the PFY vehicle, the large tail fins that incorporated the slender rear wipers were retained to make the vehicle more directionally stable, although the fins were eliminated in a later version (Figure 9 below). Morelli continued his research on the car by introducing a rhomboid arrangement of the wheels to overcome the oversteering tendency of the PF”X” vehicle. He first considered an experimental chassis (Figure 10 above) where the central wheels were the driving ones and the rear wheel was without any braking device. The central axis of the experimental chassis was also equipped with an innovative “omega-shaped” suspension and, subsequently, with an acceleration detection system along the three axles of the vehicle, as well as with an automatic braking device. This experimental vehicle was also used for directional stability tests to validate a theoretical

model of the vehicle with six degrees of freedom [5]. Subsequently, in 1992, Morelli designed and built the “PRIMA” car (Figure 10 below) where the front and rear wheels were steering wheels and the central axle, with the driving wheels, were more advanced than in the previous versions. The “PRIMA” car had a  $C_x = 0.274$  and was a real research



Figure 9. The PF ”Y” Prototype of 1961 with the large tail fins (above) and in a second version where the fins were eliminated (below) tool for increasingly advanced solutions in the automotive field.

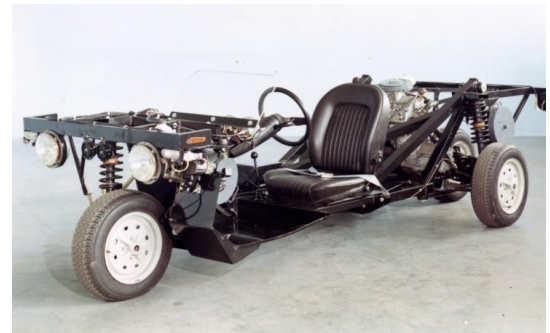


Figure 10. Rhomboid arrangement of the wheels: experimental chassis with central driving wheels and rear wheel without a braking device (above) and the “PRIMA” car (below) with front and rear steering wheels and with a central driving axle in the Pininfarina wind tunnel

## The Pininfarina wind tunnel

During the 1960s, there were only three wind tunnels in Europe that allowed real-size cars to be tested: the Daimler-Benz one in Stuttgart, initially built for aircraft, the Volkswagen one, and the MIRA one operating in the UK.

Therefore, considering the absence of a similar wind tunnel in Italy, the Italian automobile industry thought it would be opportune to build a wind tunnel for 1:1 scale vehicles.

Testing real-size cars in a wind tunnel, in addition to determining the actual aerodynamic actions while avoiding the influence of the Reynolds number, also allows various aspects of a vehicle to be controlled and tuned, such as:

- determinations of the aerodynamic components (three forces and three moments)
- visualization of the internal and external flows of the vehicle
- determination of the internal and external vehicle pressure distributions
- determination of the side wind effects on the vehicle
- measurement of aerodynamic noise, particularly inside the vehicle
- introduction of passenger compartment sealing measures
- determination of dirt deposits on surfaces while the vehicle is in motion.

Around 1965-66, Morelli carried out the preliminary work for such a tunnel for the Pininfarina company, [6,7,8, 9] on a 1:10 scale model. Some young engineers attending post-graduate courses in the Aeronautical School of the Politecnico di Torino, namely Dr. Eng. G. Ceruti and Dr. Eng. A. Cogotti, also took part in this activity (Figure 11). After these tests on the scale model, the Pininfarina wind tunnel was designed and the construction began in 1970. Construction took just under 3 years and the tunnel was inaugurated in 1972.

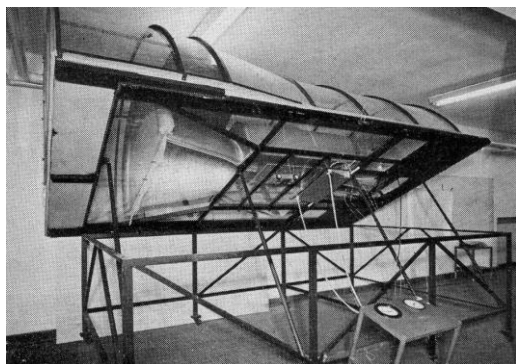
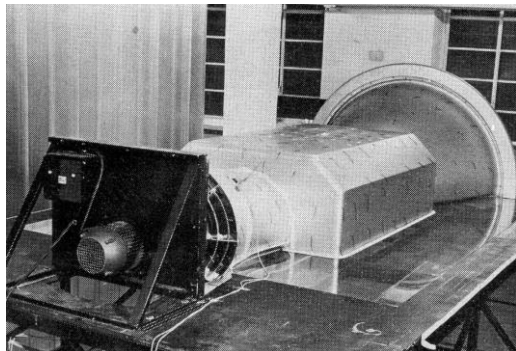


Figure 11. A 1:10 scale model of the Pininfarina wind tunnel without any exterior building (above) and with the exterior building (below) [7]

Figure 12 shows 3-D views and the longitudinal section of the final design of the wind tunnel.

At that time, the main features of this wind tunnel included:

- a 5 m diameter propeller
- a 600 HP electric motor
- a semi-open circuit with an open test chamber
- a converging part with an effusion ratio of 6.5 and a maximum speed in the test chamber of approximately 40 m/s (144 km/h)
- a diffuser downstream of the test chamber with a 1: 2 ratio
- scale with a measurement error of 1.2 ‰
- a 1500 mm dynamometric roller bench
- a return air circuit inside a specifically shaped building, with a particularly refined aesthetic aspect.

Many improvements were later made to the Pininfarina wind tunnel, for instance a higher maximum air speed of 250 km/h and a moving ground system were introduced: these improvements were possible because the basic layout of the plant and its geometric proportions had been carefully and correctly designed by Alberto Morelli.

At this point, the possibility of conducting research in the field of aerodynamics with full-scale vehicles or with scale models that were much less reduced than the previous ones, was a basic step that

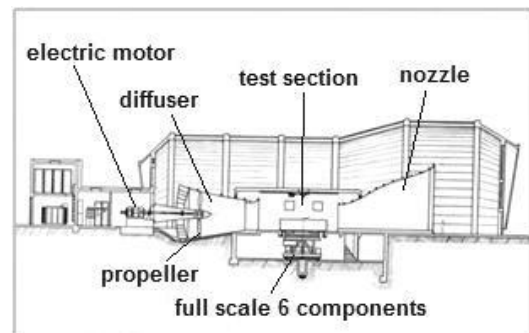
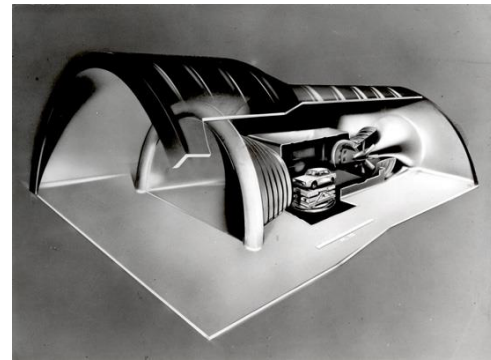


Figure 12. 3-D view (above) and longitudinal section of the Pininfarina wind tunnel with an open test chamber (below) [7]

allowed Morelli to achieve the optimal aerodynamic shape of a car that moved close to the ground, as described in the following sections.

## Comparison of aerodynamic drag tests in the wind tunnel and on the road

The first wind tunnel tests with cars in a 1:1 scale, which were already available in the early 1970s, furnished reliable results with regard to the aerodynamic coefficients, in particular for the aerodynamic drag coefficient  $C_x$ . However, systems that allowed the wheels to rotate during experimental measurements were not available in these early wind tunnels. Morelli's studies on the aerodynamics of the wheel suggested that it should not only influence the motion field around the vehicle but also its overall aerodynamic resistance [10]. An experiment that would allow the aerodynamic resistance of a vehicle to be determined under real running conditions on a road was therefore

necessary to make a comparison with the results of the wind tunnel; this research was carried out by the Politecnico di Torino and the Fiat Research Center, where a wind tunnel was also available [11]. Three medium-size European cars were selected for the wind tunnel tests, laboratory tests, and above all for the road tests, based on the coast-down method, and for the towing tests (one notchback and two hatchback cars). If a constant speed  $V$  is considered, the required power  $P_n$  can be expressed by means of the following relation:

$$P_n = A \cdot V + B \cdot V^3 \quad (1)$$

where,

$A$  and  $B$  are constants that depend on the rolling and aerodynamic coefficients, on the weight and on the dimensions, according to the following relations:

$$A = W \cdot \sin \gamma + R \quad B = \frac{1}{2} \rho \cdot C'_x \cdot S \quad (2)$$

where,

$W$  = the weight of the car

$\gamma$  = the slope of the road

$R$  = the constant part of rolling resistance

$\rho$  = air density

$S$  = a reference area of the car

$C'_x$  = a coefficient that can be expressed as:

$$C'_x = C_{xcd} + C_{xR} + C_{xo} \quad (3)$$

where,

$C_{xcd}$  = the coefficient of the aerodynamic drag

$C_{xR}$  = the coefficient of the quadratic part of rolling resistance

$C_{xo}$  = the coefficient of the drag due to the ventilation effect of the rotating parts (mainly the wheels).

In this case  $C'_x$  depends on the aerodynamic drag of the car  $C_{xcd}$ , on quadratic part of rolling resistance  $C_{xR}$  and on  $C_{xo}$ , due to the ventilation effect of the rotating parts (mainly the wheels). The  $C'_x$  coefficient and  $R$  were determined by means of coast-down tests in which the following analytical model was assumed:

$$m' \cdot \frac{dV}{dt} = A + B \cdot V^2 \quad (4)$$

where,

$m'$  = the effective mass of the vehicle (static mass plus an added mass due to the rotating parts)

$dV/dt$  = vehicle acceleration

Distance " $s$ " traveled by the vehicle as a function of time " $t$ " can be obtained from the double integration of relation (4), according to the following equation:

$$s = \frac{2 \cdot m'}{\rho \cdot S \cdot C'_x} \cdot \ln \left[ \cos \left\{ \arctan \left[ \left( \frac{\rho \cdot S \cdot C'_x}{2 \cdot A} \right)^{\frac{1}{2}} \cdot V_o \right] - t \cdot \left( \frac{\rho \cdot S \cdot C'_x \cdot A}{2 \cdot m'} \right)^{\frac{1}{2}} \right\} \right] + s_o \quad (5)$$

where,

" $s_o$ " = constant, which can be obtained for " $t = 0$ " and " $s = 0$ "

" $s$ " was measured by means of a high precision Radar-Doppler instrument, with a space interval of 100 m, for a distance of a kilometer per run and a number of runs varying from 35 to 45 for each car. A statistical analysis of the results supplied the average values of both  $R_{mean}$  and the  $C'_{xmean}$  coefficient, as shown for each car in Table 1. In order to subtract the contributions of the terms due to the ventilating effect of the wheels and the quadratic term of rolling

Table 1. Comparison of the drag coefficient values obtained from coast-down tests ( $C_{xcd}$ ) and from wind tunnel tests ( $C_{xwt}$ ) for the three types of cars taking into account the ventilation effect of the wheels ( $C_{xo}$ ) and the quadratic term of the rolling resistance ( $C_{xR}$ ) [11]

CAR	$R_{mean}$ [N]	$C'_{xmean}$	$C_{xo}$	$C_{xR}$	$C_{xcd}$	$C_{xwt}$
A	150.8	0.618	0.0119	0.0511	0.555	0.557
B	139.8	0.519	0.0116	0.0504	0.457	0.458
C	149.1	0.456	0.0116	0.0604	0.384	0.378

resistance from  $C'_{xmean}$  other rolling resistance tests were performed, that is, towing tests with the vehicle enclosed in a casing, such as that shown in the Figure 13. No aerodynamic drag of the car was measured during this test, and only the rolling resistance, the resistance of the wheel bearings, the transmission drive-line resistance in a neutral position and the air ventilation resistance due to rotation of the wheels and other parts were measured.

The last three resistances were determined through auxiliary indoor tests to also take into account the load effect. The contributions of the total ventilation resistance coefficient  $C_{xo}$ , of the rotating parts and the rolling resistance coefficient  $C_R$ , which depends on the quadratic part of the rolling resistance, are shown in Table 1. Therefore, the aerodynamic drag coefficient  $C_{xcd}$  was determined, through a coast-down test, by means of relation (6):

$$C_{xcd} = C'_x - C_{xR} - C_{xo} \quad (6)$$

At this point, wind tunnel tests were needed for the same cars that had been fully equipped and tested on the road to compare the thus obtained  $C_{xwt}$  with the  $C_{xcd}$  coefficient determined in the coast-down tests. Finally, a comparison was made between the values of the two coefficients reported in Table 1 and their  $\Delta C_x$  % percentage difference: it can be seen that the difference was very small. No investigations were carried out on the effects of a turbulent flow on



Figure 13. Trailer used to determine the rolling resistance of a vehicle [11]

the aerodynamic drag coefficient because low turbulence and calm air were chosen in the wind tunnel, as well as for the road tests.

The results of the coast-down tests were reliable as the number of tests was sufficiently high for a statistical analysis to be made, due to the high variability of the resisting forces over time.

The experimental analysis of the resistance of a car to motion through coast-down tests was of great importance to determine the  $R$  and  $C'_x$  parameters used to create the EPA FTP cycle in the USA in the early 1970s and, subsequently, in other countries.



## Other studies on the body shape of minimum drag

Morelli continued his theoretical and experimental studies on body shapes that provided even less aerodynamic drag.

The aim of this research phase was to reduce the aerodynamic resistance of a car by mainly acting on one of the three terms that constitute the total resistance, i.e. on the induced resistance, while keeping the shape resistance as low as possible, since the friction resistance only contributes very slightly. The determination of the lift distribution on a vehicle, which Morelli had already proposed in 1964 [12,13], was fundamental for this purpose.

This choice was probably due to the "aeronautical" training that Morelli had acquired in the Aerospace Engineering School and through his study, research and design activities at the Gliding Center at the Politecnico di Torino. The main aspects of this research are summarized hereafter.

The simplifying assumptions underlying this calculation are:

- perfect fluid
- the sections of the vehicle normal at velocity  $V_\infty$  of free stream are reduced to a straight-line segment parallel to the ground that pass through the center of the area of the section itself, (Figure 14 c)
- the presence of the ground is taken into account by placing a surface symmetrical to that simulating the vehicle with respect to the road surface; in this way the fluid current is parallel to the road.

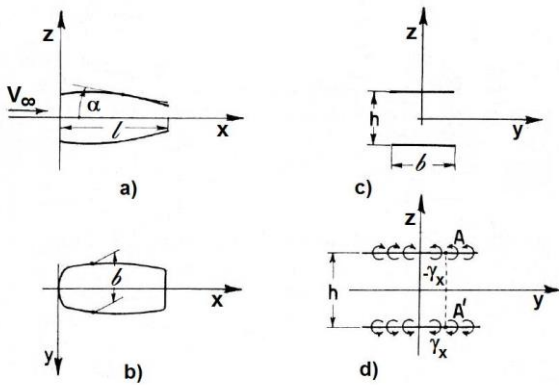


Figure 14. Schema of the reduction of the vehicle-ground system for the x,y and z axes [12,13]

Figure 14 shows the schema of the reduction of the vehicle-ground system for the x,y and z axes. Figure 14 a) shows that, for  $y = 0$ , the angle of attack  $\alpha$ , between velocity  $V_\infty$  and the profile, only depends on  $x$ . The generic section  $x = \text{constant}$  shows that width "b" and height "h" between the segment itself and its reflection only depend on  $x$ .

Finally, other hypotheses were also made:

- height "h" is small compared to the length "l" and width "b" of a vehicle
- the sine or the tangent of  $\alpha$  can be mistaken for the angle of incidence itself.

Vortexes of intensity  $\gamma_x$  are distributed on each surface to comply with the boundary conditions of two surfaces considered to simulate the vehicle-ground system, and thus the last hypothesis is introduced:

- the speeds induced in the  $x = \text{constant}$  plane are only a function of the circulation per unit of length  $\gamma_x$  in the same plane  $x = \text{constant}$  (Figure 14 d)).

For the sake of brevity, only the results of previous discussion are reported here, but the reader can refer to references [12,13] for more details. The final equation, (7), with reference to Figure 14, shows

the difference between the upper and lower surfaces of lift coefficient  $C_z$ , calculated as follows:

$$\Delta C_z = -2 \frac{\partial}{\partial x} \left[ \frac{\alpha}{h} \left( y^2 - \frac{b^2}{4} \right) \right] = -2 \left( y^2 - \frac{b^2}{4} \right) \cdot \frac{d}{dx} \frac{\alpha}{h} + \frac{\alpha}{h} b \frac{db}{dx} \quad (7)$$

The integration of equation (7) between  $\pm b/2$  (full width) and then between 0 and "l" (full length), leads to the determination of the total lift of the vehicle. The aerodynamic pitching moment can also be calculated, for example, around an axis of the  $x = 0$  plane parallel to  $y$ . Experimental tests were performed on five different car models in the wind tunnel to determine the pressure difference  $p - p_\infty$ , where  $p$  is the pressure measured at various points on the longitudinal centerline on the upper and lower surfaces, and  $p_\infty$  is the pressure of the undisturbed upstream current, as shown in Figure 15 (above); the difference in the lift coefficients from the experimental tests are instead shown in Figure 15 (below) by means of a dotted line. It is then possible to obtain the theoretical values on the centerline of  $\Delta C_{zmax}$  that are shown in Figure 15 (below) from equation (7), setting  $y = 0$ , and from equation (8) (solid line).

$$\Delta C_{zmax} = \frac{b^2}{2} \cdot \frac{d}{dx} \frac{\alpha}{h} + \frac{\alpha}{h} b \frac{db}{dx} \quad (8)$$

Observing Figure 15, it can be noted that the theoretical method in general provides a trend that is in good agreement with the experimental zone that has a positive lift. In the zone with a negative  $\Delta C_{zmax}$ , the theory instead provides a more limited region in the longitudinal direction and results in much higher maximum values than the experimental ones. As far as the front part of the car model is concerned, the reason for these differences between the theoretical and experimental values, in addition to the hypothesis introduced concerning the absence of energy losses, could also depend on the fact that the windscreen in the models used in the wind tunnel did not fit the engine hood perfectly. Instead, the differences are lower, although appreciable, in the zone where  $\Delta C_{zmax} < 0$ .

In fact, there is a stagnant area at the bonnet-windshield passage that generates a lower deflection than the flow that the boundary conditions impose.

Similar behavior was also found in four other wind tunnel tests related to the same number of car models. Morelli's theoretical determination of the lift distribution on a vehicle was not only of fundamental importance to arrive at a basic body with minimal power near the ground, but also useful in the design phase of the shape of a car body for the following reasons:

- it makes it possible to foresee the variation of the load on the wheels according to the speed
- the most suitable points for the air intakes can be identified
- useful indications are provided on the resistance coefficient of the vehicle, which is associated with the high-pressure variations along the current lines
- it is possible to identify the parameters that influence the vehicle design the most from an aerodynamic point of view.

### The body shape of minimum drag

The purpose of the research presented by Morelli in [14,15] was to achieve a body shape with minimal aerodynamic resistance (minimum total drag coefficient  $C_x$ ) by reducing the shape effects on drag



(reduced drag shape coefficient  $C_s$ ) and obtaining a zero induced drag ( $C_i \cong 0$ ), that is, the resistance due to the lift force components parallel to the oncoming flow (see formula (9)).

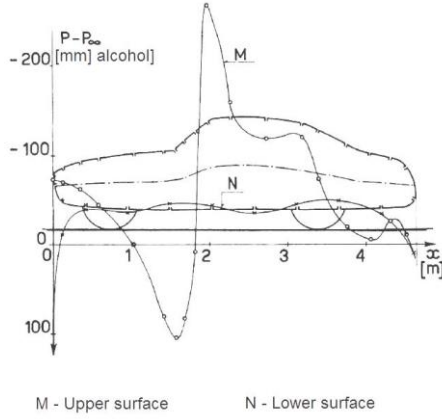


Figure 15. Pressures on the upper and lower surfaces along the centerline (above) and  $\Delta C_{zmax}$  from the experimental tests and from equation (8) (below) [ 12,13]

The third term,  $C_f$ , of total drag coefficient  $C_x$ , i.e. the friction drag coefficient, is in fact not very important and is the smallest in formula (9).

$$C_x = C_f + C_s + C_i \quad (9)$$

This conclusion can be explained on the basis of the following considerations [16].

Drop-shaped body “I” in Fig. 16 is shown with different length percent: for each length, the body presents a “clean cut” or a gradual reduction.

The body with a “clean cut” shows a higher  $C_x$  (solid line) than that of the gradual reduction (dotted line); this difference is only due to the form resistance and not to any induced resistance caused by the axial symmetry of the body, for which the lift is equal to zero.

The low aspect ratio wing portion with a camber of body “II” close to the ground shows exactly the opposite behavior: The  $C_x$  coefficient is lower for the “clean cut” solution, due to the presence of a higher induced drag in the body with a gradual reduction, despite the lower shape resistance in the latter case (the friction resistance being negligible in both cases).

Morelli then designed a new basic body under the hypothesis of:

- a total aerodynamic lift equal to zero
- gradual variation of the cross-sectional areas
- gradual variation of the shape of the oval contour of the cross sections
- null pitching moment for stability reasons

– oval contour of the transverse sections of the body.

As far as the camber of the centerline is concerned, on the basis of the results shown in Figure 3, the adopted value was 6.5%.

Therefore, in order to satisfy the condition of zero lift the distribution of  $\Delta C_{zmax}$  for the basic body (a') in figure 17, was imposed, according to equations (10) and (11):

$$\Delta C_{zmax} \cong \frac{3}{2} \Delta C_{zmed} = \frac{3}{2} \frac{1}{b} \int_{-b/2}^{b/2} \Delta C_z dy \quad (10)$$

where  $C_{zmax}$  in each cross section is approximately 1.5 times the average value of the same section.

With reference to Figure 14, the total lift,  $Z$ , can be expressed as:

$$Z = \frac{1}{2} \rho V^2 \int_0^l \int_{-b/2}^{b/2} \Delta C_z dx dy$$

and consequently

$$Z \cong \frac{1}{2} \rho V^2 \cdot \frac{2}{3} \int_0^l \Delta C_{zmax} b dx = 0 \quad (11)$$

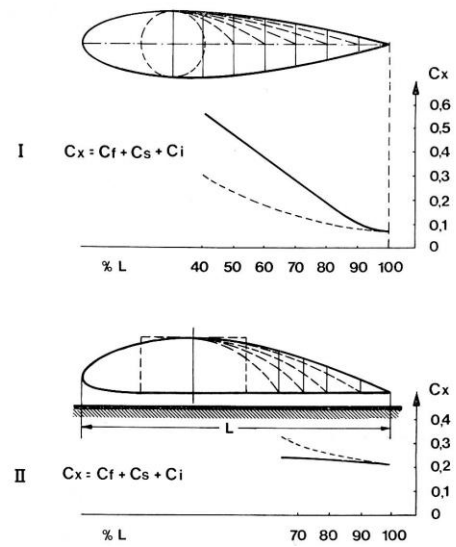


Figure 16. Drag coefficient,  $C_x$ , of an isolated “drop-shape” body, “I”, (minimum drag coeff.  $C_x \cong 0.045$ ) and of a cambered profile near the ground, “II”, for a different length % “L” [16]

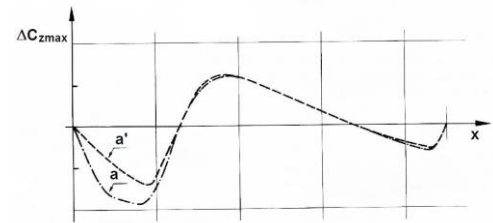


Figure 17. Theoretical lift distribution,  $\Delta C_{zmax}$ , imposed for the basic body (a') and the lift distribution of the actual body (a) [14,15]

and similarly, for pitching moment  $M$ , which is also imposed equal to zero:

$$M = \frac{1}{2} \rho V^2 \int_0^l \int_{-b/2}^{b/2} \Delta C_z \cdot x \cdot dx dy + X \cdot H \cong$$

$$\cong \frac{1}{2} \rho V^2 \cdot \frac{2}{3} \int_0^l \Delta C_{zmax} b \cdot x \cdot dx + X \cdot H = 0 \quad (12)$$

where  $X$  is the total drag and  $H$  is the height of  $X$  from the ground. Figure 17 also shows the lift distribution,  $\Delta C_{zmax}$ , for the actual body (a), while Figure 18 shows the reference axes adopted for the theoretical determination of  $\Delta C_{zmax}$ .

The lift distribution shown in Figure 17 also needs to satisfy other conditions to minimize the energy losses of the fluid:

- the negative gradients of the  $\Delta C_{zmax}$  curve should be lower than the positive ones
- there should be a minimum number (three) of the pseudo half-waves of the  $\Delta C_{zmax}$  curve.

Finally, Figure 19 shows the projections of the base body and of the actual body on the ground together with the cross-section areas. The main differences are:

- the basic body is more tapered at the ends in the plane as the cross section areas were varied according to a “drop-shape” camberd profile
- the actual body has front and rear protrusions to house the wheels and suspension
- the actual body is shorter at the front and rear for the air intake and to reduce the overall length of the vehicle.

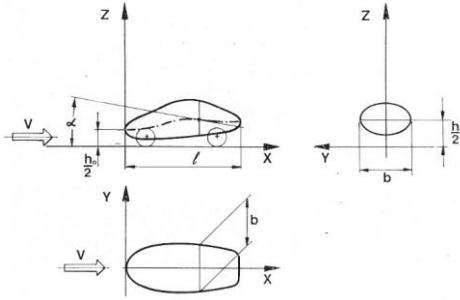


Figure 18. Reference axes adopted for the basic body for the theoretical determination of  $\Delta C_{zmax}$  [15,16]

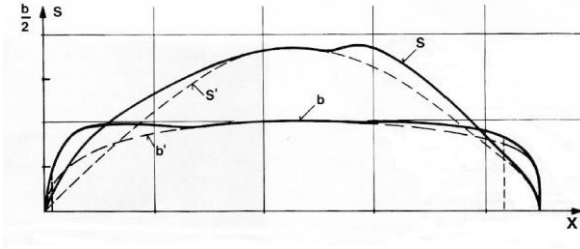


Figure 19 Width and cross-section area distributions for the basic body ( $b'$ ,  $S'$ ) and for the actual body ( $b$ ,  $S$ ) [14,15]

### Theoretical definition of the camberline

From equation (7), considering  $db/dx=0$ , as the variation of  $b$  along the  $x$  axis is practically negligible, and from the reference axes in Figure 18, the local lift coefficient can be written as:

$$\Delta C_z = -2 \frac{d}{dx} \left[ \frac{\alpha}{h} \left( y^2 - \frac{b^2}{4} \right) \right] \quad (13)$$

where,

$$\alpha = -\frac{1}{2} \frac{dh}{dx} \quad (tg \alpha \cong \alpha)$$

$\frac{h}{2}$  = height of the camberline from the ground

$$\text{If } y = 0 \quad \Delta C_{zmax} = \frac{d}{dx} \left( \frac{b^2}{2} \cdot \frac{\alpha}{h} \right) \quad (14)$$

The integration provides:

$$\frac{\alpha}{h} = \frac{2}{b^2} \int_0^x \Delta C_{zmax} dx \quad (\text{const.} = 0)$$

$$\text{and as } \frac{\alpha}{h} = -\frac{1}{2h} \frac{dh}{dx} = -\frac{1}{2} \frac{d}{dx} \ln h$$

the following is obtained:

$$\frac{d}{dx} \ln h = -\frac{4}{b^2} \int_0^x \Delta C_{zmax} dx = F(x) \quad (15)$$

By integrating the previous equation, camberline  $h$  is determined:

$$h = h_0 e^{\int_0^x F(x) dx} \quad (16)$$

where,

$$h = h_0 \text{ if } x = 0$$

An iteration, in which they  $\Delta C_z$  peaks are changed, is necessary to obtain the desired camber. In order to compare the results obtained from relation (16) with the experimental results, the basic body and the one with wheels in a 1:2 scale were tested in the wind tunnel, as shown in Figure 20.

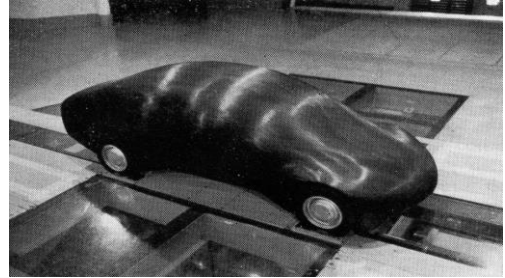
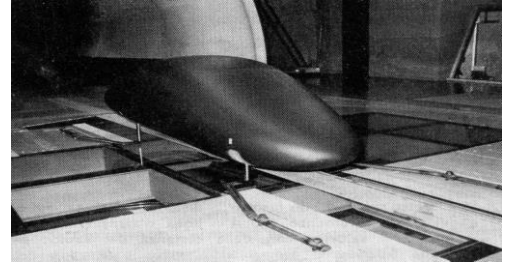


Figure 20. Basic body model ( $C_x = 0.071$ ) (above) and wheeled body model ( $C_x = 0.177$ ) (below), 1:2 scale, in the Pininfarina wind tunnel used for experimental tests [15,16]

The lift distribution of the two models is also shown in Figure 21 for the theoretical and experimental results.

A fairly good agreement between the calculated and experimentation values in can be observed Figure 21, although the negative lift in the front part is too high, as is the positive one in the central part. The pressure gradients at the back are also excessively high. However, the resistance values obtained in the tunnel were satisfactory, that is,  $C_x = 0.071$  and  $C_x = 0.177$  for the basic body and for the one with wheels, respectively.

Figure 22 shows the aerodynamically optimized basic body and the real vehicle schema that allow the mechanical needs and the housing of the occupants to be satisfied.

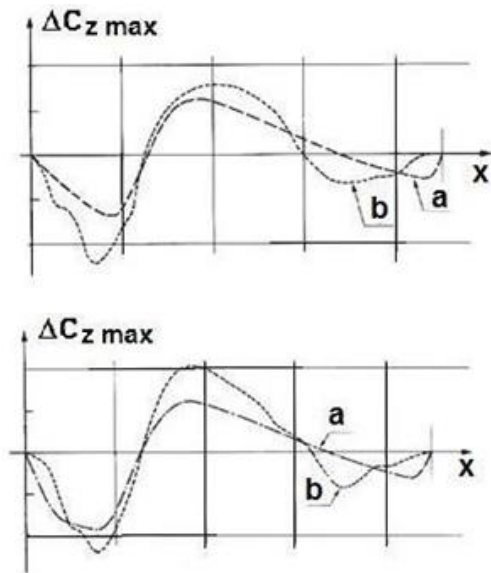


Figure 21. Comparison of the theoretical (a) and experimental (b) lift distribution for the basic body (above) and for a wheeled body (below) [15,16]

The engine and transmission can be placed in the front, while the boot can be placed in the rear. Finally, it should be noted that the width of the vehicle almost coincides with that of the wheels, distance "a" of the driver from the windscreen is acceptable, and the rear part (tail) of the "cambered" profile near the ground, as shown in Figure 16, can be reduced without any significant increment of resistance. For example, for a  $C_x$  increase to obtain a length reduction of  $\Delta TL$ , the  $\Delta C_x$  is + 0.014.

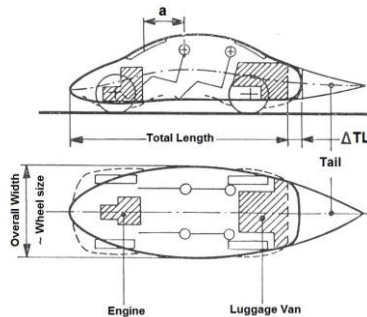


Figure 22. The aerodynamically optimized basic body and the real vehicle schema [16]

At the conclusion of this first part of this Alberto Morelli's research, some considerations, related to the energy saving obtainable from the reduction of the aerodynamic resistance of the vehicles, can be drawn. For example, under the hypothesis that the car would be used for 18% in urban traffic, for 32% in interurban traffic and for 50% on motorways, the energy waste induced by the aerodynamic drag would amount to ~ 33% of the total, with a reduction of about 50% of aerodynamic drag coefficient  $C_x$ , that is, from 0.40 to 0.20 (see Figure 6 for the year 1975/1976), and energy expenditure would decrease by about 16% [17].

## Low drag bodies moving close to the ground

After this first part of his research on the resistance of the aerodynamic drag of vehicles, Morelli continued this study and conducted

experimental tests as part of the Energy Finalized Project, Traction Subproject, Theme E "Aerodynamic improvement of vehicles", which was financed by the Italian National Research Council in the mid-seventies [18]. This project basically arose as a result of the measures adopted by OPEC following the 1973 Middle East crisis, which caused a sharp increase in the price of crude oil as well as an embargo on European countries. This interruption of the flow of oil supplies to importing nations caused problems for the economic development of the West, which, for the first time, was forced to face the problem of energy saving. Therefore, with the same criteria set out in [14,15], Morelli designed three basic bodies with different camber values, that is, 3.7%, 5.3% and 6.9%, in order to determine the lowest aerodynamic resistance near the ground [19]. Figure 23 (above) shows, as an example, the basic body profile with a camber value of 5.3% and the corresponding plan view (above). In this case, the plan form is approximately rectangular in order to meet the needs of a vehicle with a conventional arrangement of the mechanical parts. The transverse section results in a gradual varying elliptic shape that also involves the areas. Figure 23 (below) shows one of the three basic bodies during a test in the Pininfarina wind tunnel.

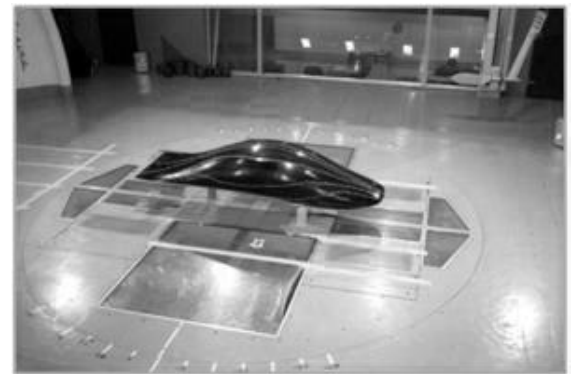
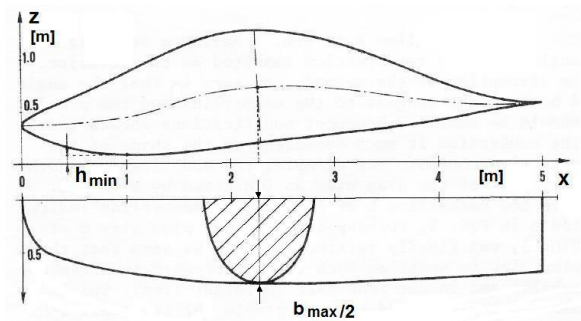


Figure 23. Basic body with a camber value of 5.3%, the corresponding plan form and an elliptic transverse view (above). The 1:2 scale model during the experimental tests in the Pininfarina wind tunnel is also shown (below) [19]

The experimental tests in the wind tunnel were carried out for each base unit with the three camber values, considering different minimum relative distances  $h_{min}/b_{max}$  from the ground (see Fig.23), and multiple angles of attack (incidence). Table 2 shows the main results as regards the value of the minimum resistance coefficient  $C_x$  obtainable for each set-up: the lowest value of  $C_x$  is just above 0.05, that is, it is comparable with the best value obtainable from an axial-symmetric streamlined body in free air. Figure 24 shows the basic body in full scale, modified on the basis of the previous considerations summarized in Figure 22. This aerodynamic shape was awarded the "Compasso d'Oro" in 1979 in recognition of Morelli's outstanding scientific work that had led to such a marked reduction in aerodynamic drag.



The “Compasso d’Oro” prize is an important recognition that is awarded by the Italian Industrial Design Association with the aim of rewarding and enhancing the quality of Italian design. It is the oldest and most prestigious industrial design award in the world.

Table 2. The main results pertaining to the value of the minimum resistance coefficient  $C_x$  obtainable for each set-up [20]

Camber %	$d = h_{\min}/b_{\max}$	$C_{x\min}$
3.7	0.20	0.049
5.3	0.1- 0.2	0.055
6.9	0.1- 0.2	0.067



Figure 24. The Pininfarina-CNR Study, 1978: which received the “Compasso d’Oro” Award in 1979

As a conclusion to this part pertaining to “the body shape of minimum drag”, Figure 25<sup>1</sup> shows the Pininfarina-CNR Study with front air intakes, internal flows as well as other details, such as rear view mirrors: the  $C_x$  value in this case was 0.20.

These scientific results were presented at the General Seminar of the Operational Units of the Energy-CNR Finalized Project, Sub-project Traction, Theme E: Aerodynamic Improvement of Vehicles, in June 1979 [19]. Here are the conclusions related to the previous issue: “*This Theme was one of the fortunate cases in which the activity was carried out extremely satisfactorily, both in terms of results and timing, and where the enthusiasm and ability of the various operating units, as well as the close connection created between them, have allowed the modeling to be consolidated with the support of experimental tests and various research activities to provide precious and complete elements for any industrial developments*”.

The words of the President of the CNR, during that General Seminar of the of the Energy Finalized Project, were both significant and prophetic: “*This historical period is characterized, not surprisingly, by science and research. The traditional structures, including scientific ones, which are called upon to renew themselves through procedures to make a qualitative leap that will place them at the forefront in a society undergoing structural changes that certainly contribute and will contribute to the improvement of the quality of life, if Scientific Research and Scientific know how are used to find the most appropriate solutions to the great crisis of our century, the energy crisis.*”

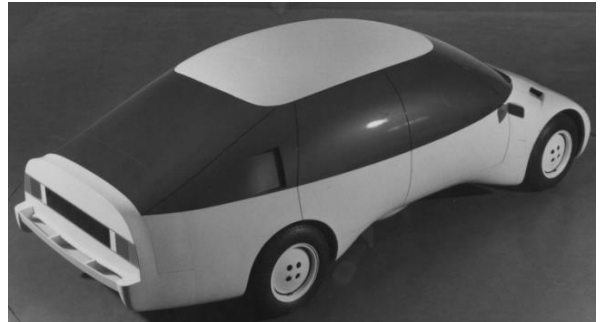


Figure 25. The Pininfarina-CNR Study with front air intakes, internal flows, rear view mirrors and other body details:  $C_x = 0.20$

## Study of aerodynamic effects on car wheels

The importance of the flow field generated by the wheels of a vehicle on the aerodynamic drag coefficient was already obvious in Morelli’s first studies. The possibilities of drag reductions for the  $C_x$  of a vehicle, as obtained from wind tunnel tests, are shown in Figure 26: a mudguard firing of the rear wheels and the profiling of the disc-wheel can lead to a reduction in aerodynamic resistance of almost 10%. Similar results were also obtained by introducing a fairing on the lower part of the chassis: however, in these experiments, the wheels did not rotate [20]. After the previous research, Morelli studied aerodynamic actions on a rolling wheel [20], where the resistance forces, lift and yaw with the three moments of rolling, pitching and yawing were measured. Figure 27 shows the test rig used for the aerodynamics study on a wheel in the wind tunnel of the Aerodynamics Laboratory at the Politecnico di Torino. The electric motor N rotates the wheel so that the air speed near the contact area on the ground, P, is zero. The wheel penetrates a space created on the ground by a few millimetres in order to simulate its deformation, but without any contact. Furthermore, wheel cover S can be modified over distance H in order to simulate different covering conditions. The entire structure is then connected to fixed crossbar T, which, in turn, is set to the wind tunnel scale.

The results related to the aerodynamic resistance and lift of the wheel along the x and z axes (Fig. 28) are defined as in equations (17) and (18):

$$X = \frac{1}{2} C_x \cdot \rho \cdot V^2 \cdot S_o \quad (17)$$

$$Z = \frac{1}{2} C_z \cdot \rho \cdot V^2 \cdot S_o \quad (18)$$

where,

$C_x$  = the aerodynamic drag coefficient

<sup>1</sup> From website: <http://www.archivioprototipi.it/carrozzeri/pininfarina/cnr.html>

$C_z$  = the aerodynamic lift coefficient  
 $\rho$  = the air density  
 $V$  = the air speed  
 $S_o$  = the projection area of the wheel on a diametric plane ( $0.135 \text{ m}^2$ ).

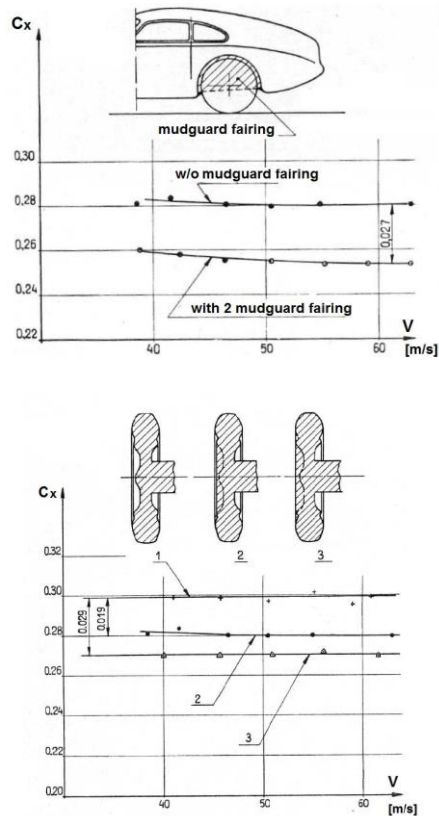


Figure 26. Significant wheel  $C_x$  reductions obtained by covering the wheel that extends from the mudguard (above) and by the profiling of the wheel disc (below) [20]

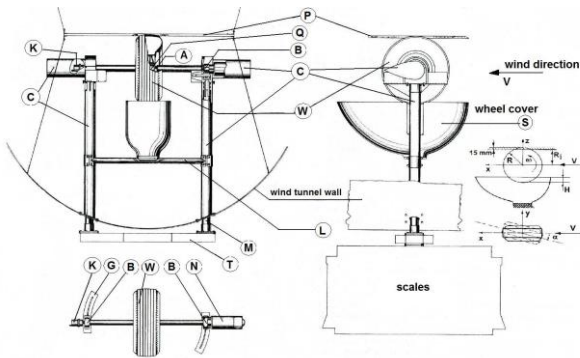


Figure 27. Test equipment in a wind tunnel for aerodynamic research on wheels: A - transmission shaft; B - ball bearing; C - cover; G - circle-arc guide; K - tachometer; L - mobile crossbar; M - vertical support; N - electric motor; P - ground; Q - wheel hub; S - wheel cover; T - fixed crossbar connected to the wind tunnel scale; W - wheel being tested [20]

Figure 28 (above) shows  $C_x$  vs incidence  $\alpha$  for different  $H$  values and for an air speed of 31 m/s: a reduction in  $C_x$  is visible when  $H$  increases; in this case, the value of  $C_x$  always refers to the initial area,  $S_o$ .

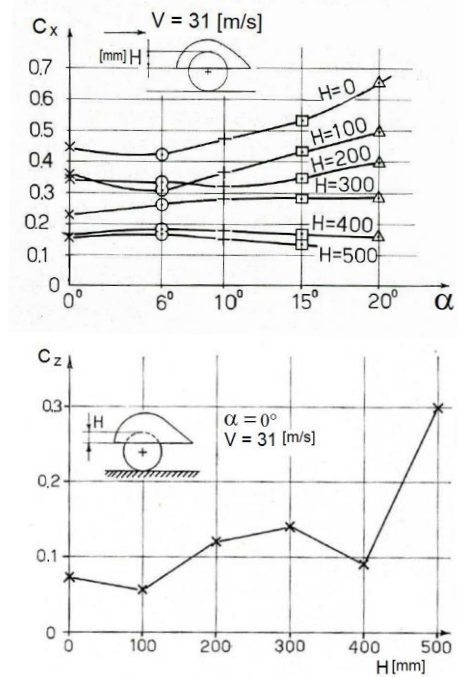


Figure 28.  $C_x$  vs incidence  $\alpha$  for different  $H$  values at  $V = 31 \text{ m/s}$  (above);  $C_z$  vs  $H$  at  $\alpha = 0^\circ$  and  $V = 31 \text{ m/s}$  (below) [20]

The aerodynamic lift coefficient  $C_z$  vs  $H$  is also shown in Figure 28 (below) for 31 m/s, with  $\alpha = 0^\circ$ : the negative lift grows as  $H$  increases (the  $z$  axis is pointing downward), that is, when the wheel cover increases. This effect leads to a marked increase in the induced resistance. This fundamental research on the aerodynamics of a wheel, and in particular on a rotating wheel, led Alberto Morelli to evaluate its effect on the aerodynamic resistance of the entire vehicle.

## Upgraded research on basic bodies

The presence of wheels can actually increase the aerodynamic drag coefficient of a car to a great extent. The aim of Morelli's research on this topic was therefore to reduce the aerodynamic interference of the wheels with the body of the vehicle by creating a non-solid diffuser, but without increasing the length of the vehicle with an unusable part. Thus, in that area, an important reduction of 30% in the shape of the car was obtained, compared to the average  $C_x$  value of the 1930's, i.e.  $C_x \approx 0.6 \div 0.65$ , as a result of the abatement of form drag coefficient  $C_s$ , as formula (9) shows. The "FIAT 127", with  $C_x = 0.48$  (1971), and FIAT "UNO", with  $C_x = 0.34$  (1983), are some examples of these vehicles. As previously mentioned, a further significant step was the reduction of the induced resistance, that is, of the  $C_i$  coefficient in formula (9), with a further decrease of  $C_x$  of 30% ( $\Delta C_x \approx 0.15$ ) from an initial value of  $C_x = 0.48$  [21].

A Notch-back Fiat "Tipo 3" car (1984) is shown in Figure 29, where  $C_x = 0.18$  was obtained by means of an induced drag coefficient of about  $C_i \approx 0$  and through a better separation of the flow in the rear part of the vehicle, that is, by reducing the form (shape) drag coefficient  $C_s$ . This result was possible thanks to a promising technology called "fluid tail technique" (FTT): the wake behind the car is considered as the end of a fluid, which allows the streamlines to meet at the back of the body.

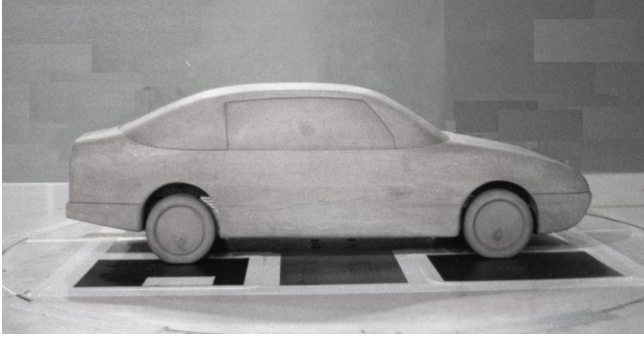


Figure 29. The Notch-back Fiat “Tipo 3” car [22,23]

These conditions are usually not present in cars, due to interference with the vortices generated by the wheels, although the fluid dynamics and geometrical conditions of the vehicle have to be present for this phenomenon to occur: a circular or elliptical base perimeter; separation of the flow along the base perimeter; constant pressure and speed conditions along the base perimeter [22,23]. As far as the interference of the vortices, generated by wheel rotation, with the wake is concerned (Figure 30), the wake cross section is at 100 mm behind the Fiat “PUNTO 75” car, where high micro drags<sup>2</sup> take place: the maximum value of  $C_{xlocal}$  ( $0.5 \div 0.6$ ) is present in a large area of the wake [22,23].

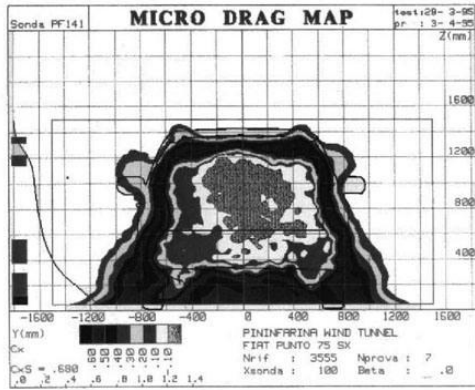


Figure 30. Micro drag map of a transverse plane 100 mm behind the FIAT “PUNTO75” car [22,23]

Cogotti [24,25] showed that a rotating wheel, in the presence of the ground, generates a system of three pairs of counter-rotating longitudinal vortices in the wake. However, research conducted at the Politecnico di Torino then showed that, if a wheel arch is present, only two jetting vortices of different intensity and one external vortex that leaves from the wheel axle are present: Figure 31 shows these two main circulation *jetting vortices*,  $\Gamma_2$  and  $\Gamma_3$ . This research conducted by Alberto Morelli also demonstrated that it was possible to reduce the jetting vortices, if a centrifugal fan were inserted into the wheel rim, as shown in Figure 32.

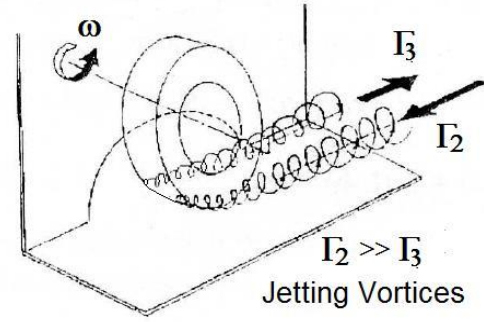


Figure 31. Main circulation jetting vortices of intensity  $\Gamma_2$  and  $\Gamma_3$  leaving the wheel

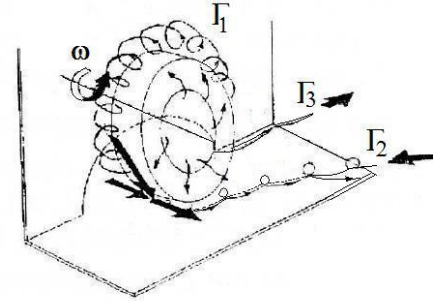


Figure 32. Reduced jetting vortices of circulation intensities  $\Gamma_2$  and  $\Gamma_3$  in the presence of a centrifugal fan in the wheel [23,24]

In order to obtain these conditions and to reduce this interference, Morelli designed, built and experimented the system shown in Figure 33, which was applied to the FIAT “PUNTO 55” car [22,23].

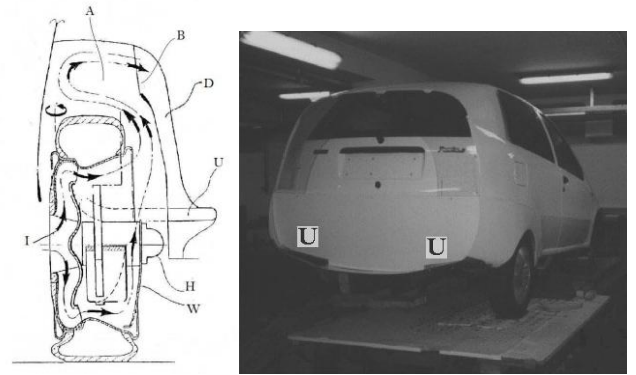


Figure 33. Modified rear wheel (left) and FIAT “PUNTO 55” car fitted with outlets “U” (right) [22,23]

<sup>2</sup> The local  $C_x$  is defined as:  $C_{xlocal} \cdot A = \int_S (1 - C_{ptot}) \cdot dS - \int_S (1 - \frac{V_x}{V_\infty})^2 \cdot dS + \int_S (\frac{V_y}{V_\infty})^2 \cdot dS + \int_S (\frac{V_z}{V_\infty})^2 \cdot dS$  where A is the sectional-cross area of the car, S is the wake section area at the plane of interest,  $C_{ptot}$  is the total pressure coefficient,  $V_x$ ,  $V_y$ ,  $V_z$  are the

components along the x, y, z axes of local speed and  $V_\infty$  is the undisturbed speed [25]



This *active aerodynamics* device involved a modification of the rear wheel aerodynamics, whereby a centrifugal fan was installed to send a sufficient flow rate (about 1/3) through input "I" to output "U", along channel "D", inside wheel arch "A". The "U" slots measured 350x20mm, and there was one for each wheel. In this way, a thin layer of air, provoked by the wheels, was created above the swirling trail: this produced continuity of the limit layer along the entire perimeter of the terminal part of the vehicle. The remaining flow rate (about 2/3) generated a vortex of intensity  $\Gamma_1$ , which remained attached to the tire until it impacted the ground, where it split into two vortices that then interfered with the jetting vortices (Figure 32). The micro-drag map in Figure 34, when compared with Figure 30, demonstrates the effectiveness of this system in a section of the wake, 270 mm behind the modified vehicle.

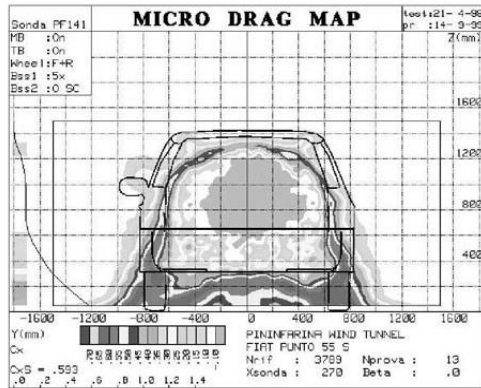


Figure 34. The micro-drag map in a section of the wake, 270 mm behind the vehicle modified as in Figure 33 [22,23]

Ultimately, the presence of the fan that sucks in air reduces the thickness of the wake, the air introduced into the wake from the rear and which exits at "U" produces a reduction in the base resistance, while the vortex adhering to tread  $\Gamma_1$  (Fig. 32) interferes with the jetting vortices by reducing their intensity and, therefore, the total car drag. As a consequence, the  $C_x$  of the modified car drops from 0.327 to 0.268, i.e. by 18 % as measured in the full-scale wind tunnel. Coast-down road tests also indicated a benefit in drag of over 20 %. This reduction in  $C_x$  resulted in a 9% increase in the maximum speed of the car and a 10% reduction in fuel consumption at 140 km/h. The thus obtained advantages were of the order of 5 kW, which should be compared with the 240 W absorbed by the rear wheels equipped with a fan.

The advantages derived from the introduction of an air flow into a current to increase its energy and improve the aerodynamic characteristics of a profile were already well known back in the 1930s. Morelli had already used this technique in the vertical tail plane of the *Veltro* glider [1,26] to improve the effectiveness of the rudder. I am convinced that that this experience of long ago, probably round about the early 1950s, was a source of inspiration for the creation of this device, which further reduced the aerodynamic drag of the car.

## The new body shape: the kompakt car (wedge Car)

Morelli continued with the FFT method he had proposed and tested on a FIAT "PUNTO" 55 with the aim of optimizing its application and determining its limits [23].

Figure 35 shows the new proposal for the body shape, which was determined on the basis of the considerations reported in [13,14], while camberline "h" was calculated by means of relation (16). The width  $b(x)$  increases gradually from the front to the rear and the base results

perpendicular to the x axis, that is, in the direction of the undisturbed air speed. Segment "Δ" (a "Cusp") was added to the rear part with the aim of creating an interface between the body and the *fluid tail*, where it operated as the first part of a diffuser that directed the flow along virtual camberline Q, without generating any lift, and minimizing the "base" resistance. The presence of the fluid tail also allowed the stationary ring vortex to be maintained, whose nucleus volume had to be as low as possible to reduce energy dissipation and increase the base pressure at the square back (a ring vortex forced the flow toward the rear part where it formed a "fluid tail").

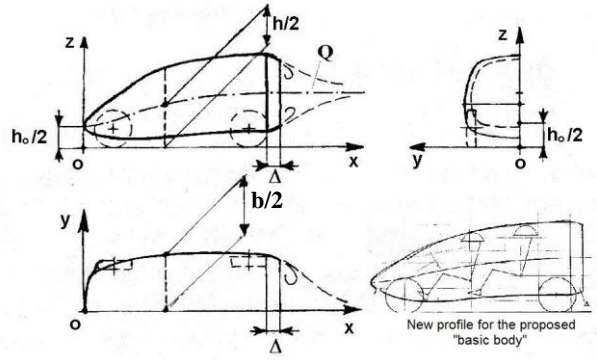


Figure 35. Reference system and the camberline of the new body shape [24]

The introduction of a fan inside the rear wheels also produced further benefits:

- improvement of the active and passive visibility in the case of rain, due to the reduced size of the trail
- reduced fouling of the rear window in the case of hatchback cars, thanks to the presence of the fluid tail
- better cooling of the brakes, thanks to the presence of wheel fairing W (Fig. 35)
- an optimum temperature of the tires could be reached earlier in city traffic (due to a greater use of the brakes, which in turn heated the air sent by the fan) and maintained during use of the highway gear, again due to the flow generated by the fan.

To the best of my knowledge, Alberto Morelli's published research in the field of automotive aerodynamics was interrupted at this point. However, his research in other fields of automotive technology, which he had always investigated, did not stop until his death in 2004.

## Conclusions

The aim of this paper has been to provide an as complete picture as possible, although succinctly, of the research activity pursued by Alberto Morelli in the field of automotive aerodynamics.

By gradually following the scientific path he made over almost fifty years, it is clear that he always attempted to interpret physical phenomena in order to innovate technology so as to improve all the different aspects of his existence, including those related to safety and environment protection.

It would therefore be an error to stop at the description of Morelli's aerodynamics activities on motor vehicles, as his studies and research covered all the different fields of automotive technology.

Scrolling through his scientific papers and the reports published in important international forums and in specialized journals, the many technical problems related to vehicles that he faced and solved emerges, as does how he went about this process. Morelli carried out extensive research in the field of automotive suspensions on the dynamic behavior of suspensions with variable flexibility, on the effects of the direction of suspension motion, thereby creating new

solutions, such as the suspension with a “Ω” shape, and he also investigated the dynamic behavior of vehicle directional and rolling stability. As far as car safety is concerned, Morelli investigated vehicle aging and set up a test system for collisions between vehicles at a reduced scale; he established a technical relationship between vehicle aging and safety, he determined the directional stability of a vehicle and also the influence of roll on tipping conditions. Moreover, he proposed a new hydraulic gearbox for the powertrain of a vehicle, which was the result of studies on the engine-power curve for vehicle traction, and a variable flywheel-mass of the crankshaft, thus demonstrating the benefits that could be achieved during acceleration and in fuel consumption.

His other research activities concerned the effects of wind on energy consumption during driving and alternative propulsion systems, such as the electric vehicle. If we consider that all this happened at the beginning of the 1990s, that is, thirty years ago, it is once again possible to understand how great Morelli's ability to precede the times was.

Alberto Morelli also designed and built a system for fatigue testing of car bodies and a tire testing machine at the then Motorization Institute. This test rig, which is still in operation at the Energy Department of the Politecnico di Torino, is provided with a flat belt on which the wheel being tested, fitted with a five-component dynamometric hub, rests, where the driving or braking torque is detected by a torque-meter located on the transmission. The characteristic angles of the wheel, camber and slip, and the vertical load are modified, thanks to a special suspension, to simulate the possible driving conditions. According to Morelli, the “*main part*” of the vehicle was the tire (he often compared it to the wing profile of an aircraft). He said that the rest came later, and all had to be done in consideration of this part. Considering the importance of tires in F1 races today, if he were here, he would say: “*You see, I was right, the tire is the first thing that has to be studied and developed*”.

Alberto Morelli was my first reference as a teacher and researcher after graduating when I started my university career in 1974 and, although officially my commitment as Assistant to Alberto Morelli in the field of Automotive Construction ended a few years later, our collaboration in teaching and at the research level continued for many more years, as I remained at the Politecnico di Torino as a professor in the field of fluid machinery until the end of my career in 2019.

Finally, I would like to conclude by also remembering Albert Morelli's long and vast educational activity, which is clearly testified by his numerous textbooks and publications [27].

## References

- Morelli A., Morelli P., “Study, construction and flight tests of high performance sailplane CVT-2 Velcro”, Proceeding of the VI OSTIV Congress, St. Yan (France) July 1956
- Morelli A., “Principali influenze sul coefficiente di resistenza aerodinamica dei veicoli”, Associazione Tecnica dell'Automobile, Breve n. 4, April 1960
- Morelli A., “Considerazioni generali sui criteri di progetto della vettura “X” Pininfarina”, Estratto dalla Rivista “Pininfarina”, Anno 2°- N. 1, March 1961, pp. 123-131
- Morelli A., “Sul comportamento in curva e in frenata di un veicolo con disposizione romboidale delle ruote”, Associazione Tecnica dell'Automobile, April 1962, pp. 131-139
- Morelli A., Perry E., Nuccio P., “On the directional stability of Motor Cars When Approaching and Exceeding the Adhesion Limits Between Tire and Ground”, FISITA Congress, Belgrade June 1986, 2<sup>nd</sup> Volume pp. 2.99-2.107
- Morelli A., “General layout characteristics and performance of a new wind tunnel for aerodynamic and functional tests on full-scale vehicles”, SAE Congress, January 1971
- Morelli A., “La galleria del vento Pininfarina per prove su veicoli in vera grandezza”, Associazione Tecnica dell'Automobile, April 1971, pp. 177-184
- Morelli A., “The new Pininfarina Wind tunnel for full scale automobile testing”, BHR - Fluid Engineering Centre Symposium, Cranfield 1973, pp. 335-351
- Morelli A., “Galleria del vento Pininfarina: studio e progetto”, Associazione Tecnica dell'Automobile, March 1974, pp. 113-129
- Morelli A., “Azioni aerodinamiche sulla ruota”, Associazione Tecnica dell'Automobile, Giugno 1969, pp. 281-288.
- Morelli A., Nuccio P., Visconti A., “Automobile aerodynamic drag on the road compared with wind tunnel tests”, SAE Congress, February 1981, Paper n. 810186
- Morelli A., “Theoretical Method for Determining the Lift Distribution on a Vehicle”, FISITA Congress, Tokyo, May 1964
- Morelli A., “Metodo teorico per la determinazione della distribuzione di portanza su di un veicolo”, Associazione Tecnica dell'Automobile, September 1964, pp. 599-606
- Morelli A., Fioravanti L., Cogotti A., “The body shape of minimum drag”, SAE Congress, Detroit, February 1976, Paper 76018
- Morelli A., Fioravanti L., Cogotti A., “Sulla forma della carrozzeria di minima resistenza aerodinamica”, Associazione Tecnica dell'Automobile, November 1976, pp. 468-476
- Koenig-Fachsenfeld R., “Aerodynamik des Kraftfahrzeugs”, Verlag der Motor Rundschau, Umschau Verlag, Frankfurt A.M, 1951
- Anticevic R., “Energia spesa nella marcia degli autoveicoli”, Associazione Tecnica dell'Automobile, November 1974, pp. 578-585
- Atti del Seminario generale delle Unità Operative del Progetto Finalizzato Energetica-CNR – Sottoprogetto Trazione. Tema E: Miglioramento aerodinamico dei veicoli. Settore: Studi per ridurre la resistenza aerodinamica. 13-16 giugno 1979, Capomulini (Catania)
- Morelli A., “Low Drag Bodies Moving in Proximity of the Ground”, ASME – Proceedings of Aerodynamics of Transportation – Niagara Falls June 1979, pp. 241-248
- Morelli A., “Azioni aerodinamiche sulla ruota”, Associazione Tecnica dell'Automobile, Giugno 1969, pp. 281-288. City University, London, November 1969
- Morelli A., “L'evoluzione aerodinamica dell'automobile”, Associazione Tecnica dell'Automobile, January-February 1988, Volume 41 n. 1-2
- Morelli A., Di Giusto N., “A new step in automobile aerodynamics – Performance improvements and design implications”, International Conference on Vehicles and Systems Progress, Volgograd State Technical University, September 1999
- Morelli A., “A New Aerodynamic Approach to Advanced Automobile Basic Shapes”, SAE Technical Paper 2000-01-0491
- Cogotti A., “A Strategy for Optimum Surveys of Passenger-Car Flow Fields”, SAE International Congress and Exposition 1989, Paper n. 890374
- Cogotti A. “Aerodynamic Characteristic of Car Wheels, Int. Journal of Vehicle Design, Special Publication SP3, 1983, ISBN 09077776019
- Morelli A., “Essais en soufflerie pour l'obtention d'une nouvelle surface de gouverne à fente”, Conférence au 7<sup>e</sup> Congrès de l'OSTIV, Juin 1958, Lezno (Pologne), Aero Revue Suisse, n. 6 1959
- Morelli A., “Progetto dell'autoveicolo-Concetti base”, Ed. CELID, December 1999, ISBN 88-7661-407-9

## **CONTACT**

Prof. Patrizio Nuccio  
Energy Department, Politecnico di Torino  
Corso Duca degli Abruzzi, 24 – 10129 Torino, ITALY  
tel.: +39-3475801069  
e-mail: [patrizio.nuccio@formerfaculty.polito.it](mailto:patrizio.nuccio@formerfaculty.polito.it)

## **ACKNOWLEDGMENTS**

The author would like to express his gratitude to the Family of Alberto Morelli for the help and support provided during the writing of this paper